



# CHORUS

This is the accepted manuscript made available via CHORUS. The article has been published as:

## Symmetry breaking in shape transitions of epitaxial quantum dots

B. J. Spencer and J. Tersoff

Phys. Rev. B **87**, 161301 — Published 11 April 2013

DOI: [10.1103/PhysRevB.87.161301](https://doi.org/10.1103/PhysRevB.87.161301)

# Symmetry breaking in shape transitions of epitaxial quantum dots

B. J. Spencer

*Department of Mathematics, University at Buffalo,  
The State University of New York, Buffalo, NY 14260-2900*

J. Tersoff

*IBM T.J. Watson Research Center,  
Yorktown Heights, New York 10598*

(Dated: March 7, 2013)

## Abstract

During heteroepitaxial growth, coherently strained islands form. These “self-assembled quantum dots” then undergo a series of shape transitions with increasing size. The best-known examples are the transitions of Ge on Si(001) and InAs on GaAs(001) from pyramidal islands to multi-faceted domes. Here we examine the transition pathway, using a simple two-dimensional model. We find that the transition occurs via sequential nucleation of individual facets. While the stable states are symmetrical, the transition states are highly asymmetrical. The calculated transition path can pass through a metastable half-dome island shape, consistent with experimental observations. The broken symmetry of the transition state can be “locked in” by intermixing with substrate material, leading to asymmetrical islands.

Nanoscale islands form spontaneously during the growth of strained heteroepitaxial semiconductor films. This process has attracted intense study as a route to self-assembly of quantum dots.<sup>1</sup> These islands are typically symmetrical in shape, but asymmetrical islands are also observed in experiment<sup>2-5</sup> and in simulations.<sup>6,7</sup> The presence of asymmetry has important implications for both the growth process and the island properties. Asymmetry in quantum dots is particularly significant for optical applications, as it can split degeneracies of quantum dot states and provide a source of optical anisotropy.

The complexity of the growth process has made it difficult to identify precisely how asymmetry arises. Both experiments<sup>2</sup> and calculations<sup>8</sup> showed that when the substrate has a modest miscut, islands can have qualitatively asymmetric shapes even in equilibrium. However, asymmetric shapes are also seen on nominally singular surfaces,<sup>3-5</sup> i.e. with the surface oriented in a high-symmetry direction.

We therefore study the energetics of heteroepitaxial islands on singular substrates, using a fully faceted two-dimensional (2D) model.<sup>8,9</sup> We focus on the transition from pyramids to domes, the two most-studied shapes for Ge and InAs islands.<sup>1</sup> For any given volume, we calculate the energies of all possible shapes. In this way we determine the entire energy surface, and the transition path and barrier heights along this surface.

As expected, with increasing island size there is a first-order transition from symmetric pyramid shapes to symmetric domes. However, we find that shape transitions occur via highly asymmetric transition states, typically involving nucleation of a steeper facet on only one side of the island. The activation barrier for this transition is much smaller than for a symmetrical transition pathway.

In addition, we find that the reaction pathway can pass through a *metastable* asymmetrical “half-dome” shape. If sufficiently long-lived, such a state could appear stable in experiment. Indeed, Ross et al.<sup>3</sup> using *in situ* microscopy clearly observed the shape transition to occur via such asymmetrical shapes by sequential nucleation of facets. Evidence of metastable half-dome states has also been observed in simulations using a 2D kinetic Monte Carlo (KMC) model.<sup>6</sup>

The asymmetrical transition state can have important consequences for the structure of the final stable island. Due to intermixing with substrate material during growth, islands typically have large internal composition gradients reflecting the growth history.<sup>4,5,7,10</sup> Thus the asymmetrical transition state will leave its mark in the composition profile. Such ef-

fects could be difficult to detect in electron microscopy (due to 2D projection) or in x-ray diffraction (which further averages over many islands). A more extreme situation can arise when intermixing drives an instability involving lateral motion of islands, which results in a highly asymmetrical composition profile.<sup>4,5</sup> It was not known what could initially break the symmetry to trigger the instability. Knowing that the symmetry is automatically broken during the pyramid-dome transition provides a natural answer to this riddle.

For our calculations we consider an isolated, completely faceted, epitaxially-strained island on a singular substrate, i.e. one exactly at a high-symmetry orientation such as Si(001). For simplicity we treat these in 2D, so the energetics are similar to extended ridges in 3D. An island shape  $y = h(x)$  then consists of  $N$  facets with orientations taken from the set of allowed facet orientations  $\theta_n$ . For simplicity we take  $\theta_n = n\theta_1$ ,  $n = 0, \pm 1, \pm 2$ , with  $\theta_1 = 2\pi/32 \approx 11.3^\circ$  to obtain an analog for the  $\{105\}$  ( $n = 1$ ) and  $\{113\}$  ( $n = 2$ ) facets found on Ge islands on Si(001). (Later we discuss the general applicability of our conclusion to 3D geometries, different facet energies and orientations, and robustness against including edge energies etc.)

Fig. 1(a) shows examples of different island types such as pyramid, half dome and dome. Island shapes  $h(x)$  are determined by minimizing the energy at fixed island volume. The total energy of an island relative to a planar epitaxial layer of the same volume is

$$E = \frac{2S_0}{\pi} \iint \ln \left| \frac{x - \xi}{a} \right| s(x)s(\xi) dx d\xi + \sum_{i=1}^N \gamma L_i - \gamma W, \quad (1)$$

where the first term is the small-slope approximation to the elastic relaxation energy<sup>11</sup> with  $s = dh/dx = \tan(\theta_i)$  (where  $\theta_i$ ,  $i = 1, \dots, N$  is the orientation of the  $i$ th facet),  $S_0$  is the elastic energy density of a planar film due to misfit,  $a$  is any convenient length scale (its value does not affect the energy because its contribution integrates to zero), and the remaining terms are the excess surface energy due to the presence of the island with surface energy  $\gamma$ , facet lengths  $L_i$  and island width  $W$ . (The surface energy in the last term is the same as the other surface energies because we assume the film wets the substrate.<sup>12</sup>) To find the equilibrium shape for a given island type with given volume  $V$ , we minimize  $E$  numerically with respect to the motion of each facet normal to itself subject to the volume constraint  $\int h(x) dx = V$ . For a given set of facets and prescribed volume, the resulting island shape has equal chemical potential  $\mu$  for each facet,<sup>13</sup> and corresponds to an energy minimum (or to some other extremum such as an unstable maxima or saddle-point solution). Our results

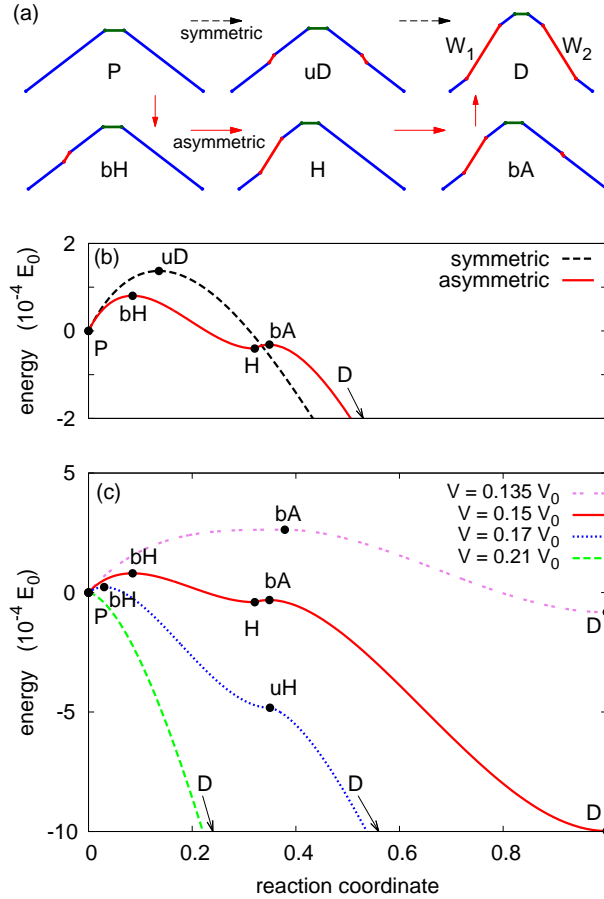


FIG. 1. (Color online) (a) Island shapes at critical points along the transition pathway at island volume  $V = 0.15V_0$ . Capital letters denote island type: pyramid (P), half dome (H), asymmetric dome (A), symmetric dome (D); lower case letters denote unstable solutions: saddle point barrier (b), local energy maxima (u). Note  $y$  scale is stretched by a factor of 4 to better show details of each shape. (b) Energy vs reaction coordinate (see text) for transition from pyramid (P) to dome (D) at  $V = 0.15V_0$ . Marked points are critical points with island shapes shown in (a). The transition pathway involving asymmetric states has lower energy barriers than the pathway involving only symmetric states. (c) Energy vs reaction coordinate for transition from pyramid to dome at different island volumes  $V$ . Values of  $V$  correspond to specific cases (c)-(f) of Fig. 2, with each curve showing the energy relative to the pyramid for that case.

are given in terms of characteristic scales for length  $l_0 = \gamma/S_0$ , 2D volume  $V_0 = l_0^2$ , energy  $E_0 = \gamma^2/S_0$ , and chemical potential  $E_0/V_0$ .

The central results of this paper are summarized in Fig. 1(c), showing the energy vs. “re-

action coordinate” for the transformation from pyramid P to dome D at different volumes. This transformation requires the nucleation of two steep facets, one on each side of the island. The reaction coordinate is defined here as the length of the steep facets [ $W_1 + W_2$  in Fig. 1(a)] relative to their length in the completely transformed dome. At all volumes where the pyramid-dome transition occurs, we find that the transition must pass through an asymmetric intermediate state.

A particularly important case is highlighted in Fig. 1(b), corresponding to volume  $V = 0.15V_0$ . The asymmetric transition pathway is shown as a solid line, with labels referring to the corresponding island shapes shown in Fig. 1(a). Nucleation and growth of the first facet corresponds to the path P-bH-H, resulting in a metastable half-dome island H. Nucleation and growth of the second facet corresponds to the path H-bA-D, ending with the formation of a symmetric dome.

The dotted line in Fig. 1(b) shows for comparison the transition pathway when symmetry is imposed. In that case the transformation from pyramid to dome requires simultaneous nucleation of a new steep facet on each side (uD). The nucleation barrier in this symmetric case,  $E(uD) - E(P)$ , is nearly twice as large as the barrier  $E(bH) - E(P)$  for the asymmetrical pathway. We show below that in all cases the pyramid-dome transition occurs via an asymmetrical pathway, typically involving successive facet nucleation events.

The results shown in Fig. 1(b) are for a fixed volume,  $V = 0.15V_0$ . To illustrate how the energy landscape changes with volume, we plot in Fig. 2 the energy vs the lengths of the two steep facets [denoted  $W_1$  and  $W_2$  in Fig. 1(a)]. For each plot in Fig. 2, the pyramid shape corresponds to the lower left corner where  $W_1 = W_2 = 0$ . Symmetric solutions lie on the diagonal ( $W_1 = W_2$ ), which is a plane of symmetry. Off-diagonal solutions are asymmetric, and solutions on the axes  $W_1 = 0$  or  $W_2 = 0$  are half domes with a steep facet on one side only. To obtain these energy surfaces, we fix the volume at the value indicated, and for each  $W_1$  and  $W_2$  we find the lengths and positions of the remaining facets that give the minimum energy.

The energy vs reaction coordinate depicted in Fig. 1(b) corresponds to a pathway in the energy landscape shown in Fig. 2(d). The dome (D) is the stable solution, lying in a deep energy minimum. The pyramid (P) is metastable, in a local energy minimum. The transition pathway with the lowest barrier, corresponding to the solid line in Fig. 1(b), is marked by the arrows in Fig. 2(d). Starting from the pyramid (P), the first step is to nucleate one

facet (bH) and then form a one-sided dome (H). This involves passing over a barrier along the boundary of the energy surface at (bH). To form the second facet, the energy barrier is a saddle point (bA) on the energy surface, corresponding to an asymmetric dome with one small steep facet and one larger steep facet. After the barrier at bA the energy decreases to the minimum point at D, a symmetric dome. The alternative symmetric pathway, the dotted line in Fig. 1(b), would correspond to a path in Fig. 2(d) traversing the diagonal P-uD-D, passing over a local energy maximum at uD. This pathway has the largest energy barrier of all critical points on the energy surface between the pyramid and dome solutions.

Comparing the different plots in Fig. 2 shows how the energy surface evolves with increasing island volume. The topography of the energy surface changes as the saddle points and local maxima and minima move, split or merge as a function of volume; and the transition pathway is qualitatively different according to the topographic features. The six plots in Fig. 2 show every distinct case for the topography of the energy surface. For each of these energy surfaces we can determine the corresponding plot of energy vs “reaction coordinate” for the transition from stable/metastable pyramid to dome. These results are shown in Fig. 1(c), where the energy for each case is plotted relative to the energy of the pyramid for that case. As Fig. 1(c) shows, all transition pathways involve asymmetric shapes, and for the range of volumes corresponding to case *d*, the asymmetric half-dome shape is metastable.

The volume dependence of the shapes, stability, and transition pathways from Fig. 2 is summarized in the bifurcation diagram Fig. 3. Figure 3(a) shows the energy vs volume for the stable, metastable and saddle-point configurations of different island types. Vertical lines and letters at the top of the figure indicate the range of volume for the different cases depicted in Fig. 2. For example, the transition via a metastable half-dome occurs for the volume range labeled *d*, via the sequence P-bH-H-bA-D, as in Fig. 2(d). It is interesting to note that this range begins slightly above the equilibrium transition volume. Because the activation barrier is much smaller in region *d* than for smaller volumes, it seems likely that during growth the island will overshoot the equilibrium transition, with the shape transition occurring only when the size reaches region *d*. Region *c* around the equilibrium transition is the only case where both steep facets nucleate simultaneously. The transition state is still asymmetrical, because the two facets have different sizes.

Figure 3(b) shows the chemical potential  $\mu$  of the solutions in Fig. 3(a). The pyramid solution has a higher chemical potential than the dome over the entire range of island volume.

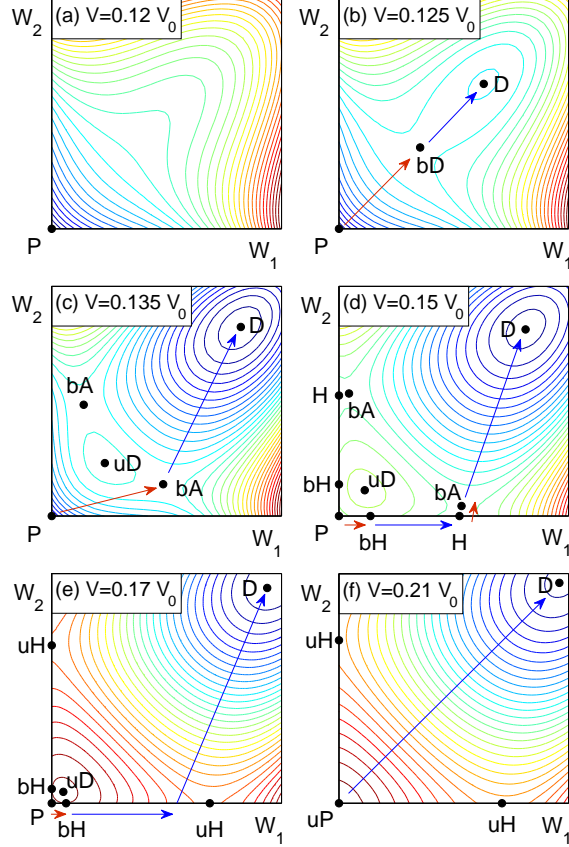


FIG. 2. (Color online) Energy surfaces as a function of the lengths  $W_1$ ,  $W_2$  of the steep facets on each side of the island. Colored contours show the energy surface with energy decreasing from red to blue. Different plots (a)-(f) correspond to increasing island volume as labeled. Note that (d) corresponds to Fig. 1(b), and (c) is the size where pyramid and dome are degenerate in energy. Marked points correspond to island types with notation given in Fig. 1. Arrows show the lowest-barrier transition pathway from P to D, with red denoting uphill in energy and blue denoting downhill in energy.

Both the dome and half dome solution curves are “C-shaped” with stable/metastable solutions on the lower portion and with barrier solutions on the upper portion. The asymmetric dome solutions exist on a short segment connecting the half-dome and dome solutions. While Fig. 3(b) does not show the relative energies of the different solutions, it more clearly shows the connections of the different solution branches, and shows that the transition sequence decreases the chemical potential monotonically and discontinuously.<sup>14–16</sup>

The kinetics of the shape transition depend on the magnitude of the energy barriers rela-



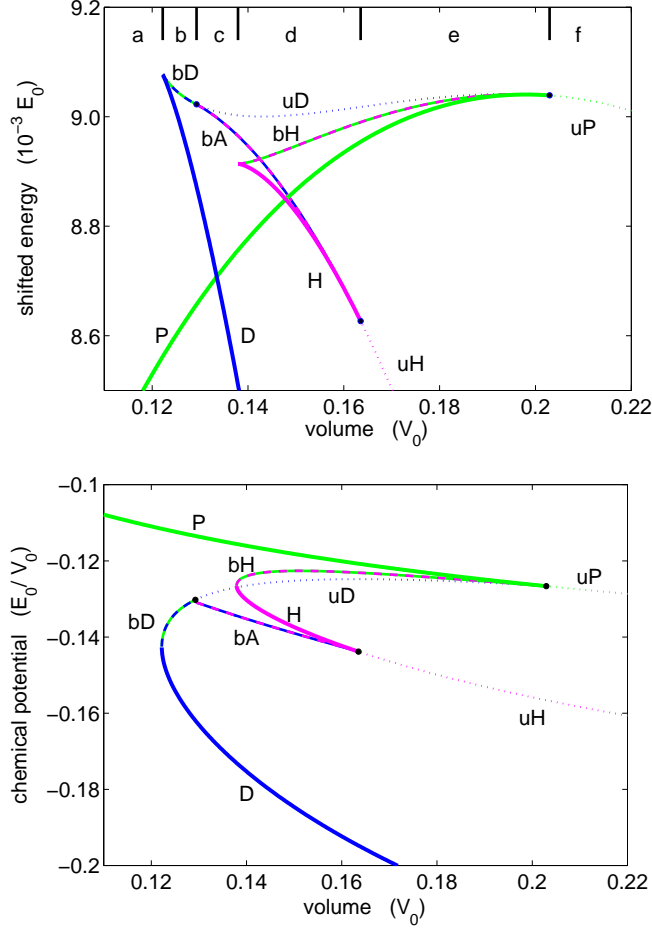


FIG. 3. (Color online). (a) Bifurcation diagram of solutions. The shifted energy  $E + 0.126S_0V$  is used so that the features of the plot are more visible. Solution types are labeled as in Fig. 1. Solid lines: stable or metastable state; dashed lines: saddle point barrier; dotted lines: unstable local energy maxima. Dots indicate bifurcation points where solution branches corresponding to different island types join. Letters a-f across the top of the figure indicate the different cases from Fig. 2(a-f). (b) Chemical potential of solutions in (a).

tive to the system fluctuations. Consider the pyramid to dome transition in Fig. 3(a) region *d*. Here, the magnitude of the first barrier P-bH is much larger than the magnitude of the barrier for the second transition H-bA. Thus, for finite fluctuations the first transition should occur much more slowly than the second. While the half-dome state H is metastable, its lifespan as a transition state will be relatively short, which could make it difficult to observe in experiment. Ross, Tromp and Reuter<sup>3</sup> do in fact observe asymmetric dome shapes in their experiments on GeSi/Si island coarsening. It is possible that a longer-lived metastable state

in experiment reflects the specific facet energies and orientation of Ge/Si, and the difference between 3D and 2D. In addition, during growth small asymmetries in the environment can develop, such as strain gradients or local misorientations, due to the presence of neighboring islands.<sup>17</sup> This could increase the lifetime of metastable configurations, making them easier to observe experimentally. Of course, in an asymmetrical environment even the ground state becomes asymmetrical, as for “miscut” crystal surfaces.<sup>2,8</sup> The key point is that, unlike the ground state, the transition is *inherently* asymmetrical, even in a perfectly symmetrical environment. Moreover, the transition may be sensitive to small environmental asymmetries that have minimal effect on the ground state.

The calculations summarized in Fig. 2 give the actual island shape associated with each of the barriers. Thus we explicitly determine the location and size of critical facet nucleus for each transition. For example, to change from pyramid to half dome, an island nucleates a relatively small “steep” facet near the middle of one of the sides of the pyramid, as shown in the bH shape in Fig. 1.

The calculations here assume a strictly faceted geometry. However, at the atomic scale, the new facet is believed to form by bunching of atomic steps<sup>18</sup> as an intermediate state before coalescing into facets.<sup>6,19</sup> This process can be seen in KMC simulations.<sup>6</sup> However, it is not clear what configuration represents the transition state in the step-bunching picture. Our work provides a continuum-theory analog of this mechanism, which sacrifices atomic-scale detail in return for the ability to explicitly address the full transition pathway at all volumes. What is most striking is the overall similarity between our theory and the KMC simulations despite the differences between step bunches and true facets.

While we present results only for a particular set of facet angles and facet energies, we expect the key conclusions to apply rather generally. In particular, we expect that the shape transition occurs via an asymmetric transition state even in a 3D model, and over a range of facet energies and orientations. For very small structures, the energies of facet edges can become important, in addition to the surface energies. We therefore have examined the effect of edge energies (corner energies in 2D) on the shape transitions by adding an energy cost  $\delta$  for each corner on the island shape. The corner energy terms result only in the upward shift of each energy curve in Fig. 3(a) by an amount corresponding to the added corner energy for each island type. While the corner energy increases the energy of the dome with respect to the half dome, it also increases the energy of the half dome relative to the

pyramid by the same amount, and so we find corner energy can not render the half dome stable. In the more general case, allowing different edge energies for different facets, and/or allowing for the steep facets to have a different surface energy than the other facets, we find the same result: the half-dome can be metastable, but can not become stable relative to the dome.

In summary, we find that strained-island shape transitions occur via asymmetric intermediate shapes, with important implications for island growth. In particular, the pyramid-dome transition can involve a metastable half-dome shape as an intermediate state. These results provide qualitative new insight into the shape evolution of heteroepitaxial islands, and shed light on a number of experimental observations.

This work was supported by an NSF grant DMS-0505497 (BJS).

- 
- <sup>1</sup> For a review, see J. Stangl, V. Holý, and G. Bauer, *Rev. Mod. Phys.* **76**, 725 (2004).
- <sup>2</sup> P. Sutter, E. Sutter, and L. Vescan, *Appl. Phys. Lett.* **87**, 161916 (2005).
- <sup>3</sup> F. M. Ross, R. M. Tromp, and M. C. Reuter, *Science* **286**, 1931 (1999).
- <sup>4</sup> U. Denker, A. Rastelli, M. Stoffel, J. Tersoff, G. Katsaros, G. Costantini, K. Kern, N. Y. Jin-Phillip, D. E. Jesson, O. G. Schmidt, *Phys. Rev. Lett.* **94**, 216103 (2005).
- <sup>5</sup> G. Katsaros, A. Rastelli, M. Stoffel, G. Isella, H. von Känel, A. M. Bittner, J. Tersoff, U. Denker, O. G. Schmidt, G. Costantini, and K. Kern, *Surf. Sci.* **600**, 2608 (2006).
- <sup>6</sup> C.-H. Lam, *J. Appl. Phys.* **108**, 064328 (2010).
- <sup>7</sup> Y. Tu and J. Tersoff, *Phys. Rev. Lett.* **98**, 096103, (2007).
- <sup>8</sup> B. J. Spencer and J. Tersoff, *Appl. Phys. Lett.* **96**, 073114 (2010).
- <sup>9</sup> I. Daruka, J. Tersoff and A.-L. Barabasi, *Phys. Rev. Lett.* **82**, 2753 (1999); I. Daruka and J. Tersoff, *Phys. Rev. B* **66**, 132104 (2002).
- <sup>10</sup> M. S. Leite, A. Malachias, S. W. Kycia, T. I. Kamins, R. S. Williams, and G. Medeiros-Ribeiro, *Phys. Rev. Lett.* **100**, 226101 (2008).
- <sup>11</sup> J. Tersoff and R. M. Tromp, *Phys. Rev. Lett.* **70**, 2782 (1993).
- <sup>12</sup> B. J. Spencer and J. Tersoff, *Phys. Rev. Lett.* **79**, 4858 (1997).
- <sup>13</sup> W. C. Carter, A. R. Roosen, J. W. Cahn, and J. E. Taylor, *Acta Metall. Mater.* **43**, 4309 (1995).
- <sup>14</sup> S. P. A. Gill and A. C. F. Cocks, *Proc. R. Soc. A*, **642**, 3523 (2006).

- <sup>15</sup> A. C. F. Cocks and S. P. A. Gill, Phys. Rev. B, **76**, 085328 (2007).
- <sup>16</sup> F. M. Ross, J. Tersoff and R. M. Tromp, Phys. Rev. Lett. **80**, 984 (1998).
- <sup>17</sup> J. A. Floro, G. A. Lucadamo, E. Chason, L. B. Freund, M. Sinclair, R. D. Twisten and R. Q. Hwang, Phys. Rev. Lett. **80**, 4717 (1998).
- <sup>18</sup> J. Tersoff, Y. H. Phang, Z. Zhang, and M. G. Lagally, Phys. Rev. Lett. **75**, 2730 (1995).
- <sup>19</sup> F. Montalenti, P. Raiteri, D. B. Migas, H. von Kanel, A. Rastelli, C. Manzano, G. Costantini, U. Denker, O.G. Schmidt, K. Kern and L. Miglio, Phys. Rev. Lett. **93**, 216102 (2004).